Archives of Mechanics • Archiwum Mechaniki Stosowanej • 26, 3, pp. 459–478, Warszawa 1974

Self-induced motion and stability of concentrated vortex filaments

S. E. WIDNALL and D. B. BLISS (Cambridge)

THE SELF-INDUCED motion and stability of vortex filaments has been investigated both theoretically and experimentally. Through an application of the method of matched asymptotic expansions, a general solution is obtained for the self-induced motion of a vortex filament containing an arbitrary distribution of swirl and possibly axial velocities. This solution has been applied to several vortex-flow stability problems: the stability of a vortex line containing an axial jet, the mutual inductance instability of a vortex pair and the instability of helical vortex filaments and vortex rings. Only the results for the vortex ring will be discussed in detail. Experimental studies of a vortex ring using a Laser Doppler Velocimeter were performed to determine the circulation and vorticity distribution within the vortex rings. Comparison of the observed vortex-ring motion and instability with theoretical predictions will be presented.

Samowzbudny ruch i stateczność włókien wirowych rozpatrywano teoretycznie i doświadczalnie. Stosując metodę odpowiednio dobranych rozwinięć asymptotycznych otrzymano rozwiązanie ogólne dla samowzbudnego ruchu linii wirowej, zawierającej dowolny rozkład prędkości wirowych i ewentualnie osiowych. Rozwiązanie to zastosować można do wielu zagadnień stateczności przepływów wirowych: stateczności linii wirowej zawierającej strumień osiowy, wzajemnej niestateczności indukcyjnej dwóch wirów, niestateczności spiralnych włókien wirowych i pierścieni wirowych. Szczegółowo omawia się jedynie pierścienie wirowe. Wykonano badania doświadczalne pierścieni wirowych za pomocą laserowego prędkościomierza dopplerowskiego dla ustalenia wirowości i cyrkulacji. Przedstawiono porównanie wyników teoretycznych i doświadczalnych, dotyczących ruchów i niestateczności pierścieni wirowych.

Автоколебательное движение и устойчивость вихревых струй рассматривались теоретически и экспериментально. Применяя метод соответственно подобранных асимптотических разложений получено общее решение для автоколебательного движения вихревой линии содержавшей произвольное распределение вихревых скоростей и возможно осевых скоростей. Это решение можно применять к многим проблемам устойчивости вихревых течений: устойчивость вихревой линии содержавшей осевой поток, взаимная индуктивная неустойчивость двух вихрей, неустойчивость спиральных и кольцевых вихревых линий. Подробно обсуждаются только кольцевые линии. Проведены экспериментальные исследования вихревых колец при помощи лазерного допплеровского скоростемера для установления завихренности и циркуляции. Будет представлено сравнение теоретических и экспериментальных результатов, касающихся движений и неустойчивости вихревых колец.

1. Introduction

IN RECENT years, there has been considerable interest in the dynamics of vortex flows in free motion. This has been inspired, at least in part, by the aircraft-wake-turbulence problem. The trailing vortices shed by large aircraft are sufficiently strong and persistent to pose a safety hazard to other aircraft operating in the vicinity. Clearly, it is desirable to understand the mechanisms by which such vortex wakes are dissipated. The trailing vortices undergo a natural sinusoidal instability which eventually causes them to touch and break into crude rings. This destroys the initial wake structure much more quickly than simple viscous decay. The character and potential hazard of the residual wake structure after the

completion of sinusoidal instability is still not well understood. Under ideal conditions, this residual structure may resemble a series of vortex rings which, depending on the circumstances and the time elapsed, may have their vorticity concentrated in a small core region or distributed throughout their volume. It is apparent, therefore, that the dynamics and stability of vortex pairs and vortex rings are of practical interest. The study of such vortex motion leads to many fundamental problems in the mechanics of incompressible, rotational flows.

The present study deals with the general problem of the dynamics and stability of curved vortex lines whose rotational core includes axial flow. The characteristic size of the core is assumed to be small compared to the local radius of curvature and all other physical lengths associated with the vortex line shape. This being the case, the core of this vortex-jet represents a region of highly concentrated vorticity. This flow configuration is relevant to the motion and stability of trailing vortices and vortex rings of small core size.

Throughout the analysis, an incompressible, inviscid, rotational flow is assumed. This is justifiable because the time scale for viscous diffusion is much slower than the time scales for the dynamics of these flows.

In the study of the dynamics of curved vortex lines with axial flow, it might be thought that an adequate model would be a curved potential vortex line with its self-induced motion calculated by the Biot-Savart law. However, it is well known that the self-induced velocity of such a vortex line is infinite due to a logarithmic singularity when the velocity is evaluated on the line itself. It is, therefore, necessary to consider the problem in greater detail and this involves studying the fluid motion in the curved rotational vortex core. This problem can be solved in a quite general manner using the method of matched asymptotic expansions. The core size of the vortex line must be much smaller than the local radius of curvature and the characteristic scale for axial variation. The order of the axial velocity must not exceed that of the swirl velocity. This solution was reported in BLISS (1970) and WIDNALL, BLISS and ZALAY (1971); it is reviewed and discussed further here. Earlier work in this area was done by TUNG and TING (1967) who considered a decaying vortex ring. MOORE and SAFFMAN (1972) have also provided a general analysis of the motion of a vortex filament with axial flow.

The motion of particular curved vortex line configurations has been the subject of classical and recent investigations. Historically, the earliest work on this subject was probably that by W. THOMSON (Lord Kelvin) who found the motion of a vortex ring and a sinusoidally perturbed vortex line for special vorticity distributions in the core, see THOMSON (1910) and LAMB (1945). Additional classical studies of the motion of the vortex ring are due to HICKS (1885) for a hollow core, DYSON (1893) for the constant vorticity core carried to fourth order, and J. J. THOMPSON (1883). More recently, using the energy method outlined in LAMB (1945), SAFFMAN (1971) found the propagation speed for a vortex ring of small core with an arbitrary swirl distribution; the additional effect of axial velocity in a ring is included in SAFFMAN (1970). The motion of steady vortex rings of small cross-section has also been studied by FRAENKEL (1972) who considers cores with arbitrary swirl distribution and carries the uniform vorticity core to higher order.

One of the important developments of BLISS (1970) is the derivation of a general formula for cut-off distance. Very often in the past, the motion of curved vortex filaments has been

approximated using the Biot-Savart integral over a curved potential vortex line and employing a cut-off distance to avoid the logarithmic singularity thus encountered. The general formula for cut-off distance depends only on the core size and the axial and swirl kinetic energy content of the core.

This general solution for self-induced motion of a curved vortex line has been applied to obtain specific results about the dynamics and stability of particular vortex configurations of particular interest.

The stability of the vortex pair as a model for an aircraft wake was first studied by CROW (1970) using the cut-off distance method. Because the general formula for cut-off distance was not then available, he based his choice of cut-off distance on the results of known classical solutions by THOMSON (1910). All the physical features of the instability were identified by CROW. BLISS (1970) and WIDNALL, BLISS and ZALAY (1971) used their general analysis to include the effects of core structure and axial flow.

Interest in the vortex-ring instability began in the late nineteenth century because of the proposal of Lord Kelvin that vortex rings in an aetherial fluid might be the basic constituent of matter. This was inspired, at least in part, by the indestructability of vortex lines in an ideal fluid. The question of stability and of possible frequencies of oscillation of vortex rings was, therefore, of considerable interest. The stability of the small core ring was investigated by THOMPSON (1883), HICKS (1885) and DYSON (1893). (Additional references are available in LAMB (1945), Article 166.) In all cases, the ring was found to be stable with disturbances rotating around the core without amplification.

There is, however, considerable experimental evidence that the vortex ring is unstable. KRUTZSCH (1939) presents photographs of the vortex ring instability with as many as twelve lobes standing and amplifying. MAXWORTHY (1972), in an experimental paper primarily on the steady structure, notes that very energetic rings can be unstable. A detailed experimental structure of the vortex ring was made by SULLIVAN (1973) who photographed the instability and used a laser Doppler velocimeter to obtain quantitative data. This work is also reported in SULLIVAN, WIDNALL and EZEKIEL (1973) and WIDNALL and SULLIVAN (1973). These papers provide the best description and quantitative information on vortex ring structure and the ring instability. The instability problem has been re-examined analytically by WIDNALL and SULLIVAN (1973) using the general formula for cut-off distance. With this approach, they find the vortex ring to be unstable with reasonably good agreement between theory and experiment. In a related problem, WIDNALL (1972) studied the stability of the helical vortex filament and identified its modes of instability.

In this paper, many of these results will be discussed.

2. Self-induced motion of a curved vortex line

For a vortex filament of small core size, the induced velocity at a point y_1 on the filament may be evaluated by a proper interpretation of the Biot-Savart law

$$\bar{q}(y_1) = \frac{\Gamma}{4\pi} \int \frac{(\bar{y}-\bar{y}_1)}{c|y-y_1|^3} x\, d\bar{y} \tag{2.1}$$

in terms of the vorticity distribution within the vortex core.

The solution and proper interpretation of (2.1) will be obtained by aid of matched asymptotic expansions. Two asymptotic solutions are sought: one approximate solution (the inner solution), valid in the limit $\varepsilon \to 0$ only within the rotational vortex core and its immediate surroundings and another approximate solution (the outer solution), valid in the limit $\varepsilon \to 0$ in all regions of the flow except the vortex core. In general, each of these solutions would contain undetermined parameters which must be found by matching. For the present problem, the small parameter ε is the ratio of vortex-core size to the local radius of curvature of the vortex line.

In the application of the method of matched asymptotic expansions to the calculation of the flow field and self-induced motion of a vortex filament, the behavior of (2.1) in the limit $r \to 0$ serves as the lowest-order outer solution. For a general vortex filament, it was found to be most convenient to construct this outer solution in terms of the cut-off evaluation of (2.1).

In the general case of the calculation of self-induced motion at a point s on an arbitrary vortex filament, cutting off the integral (2.1) a small distance l on either side of the point will produce an expression of the form

$$\bar{q}(s) \approx \frac{\Gamma}{4\pi R(s)}\left[-\ln\frac{l}{R(s)}\bar{n} + \bar{B}(s)\right], \tag{2.2}$$

where R is the local radius of curvature, $\bar{n}$ is the unit binormal and $\bar{B}(s)$ is an 0 (1) function representing the effects of distant portions of the filament.

To obtain the complete outer solution, the missing arc $\pm l$ must be added. If the coordinate system is chosen to move with the filament, the self-induced velocity $\bar{q}$ must also be included.

The problem is formulated in a local cylindrical (r, θ) coordinate system centered on the vortex core at a point s along the filament; the x-axis lies along the vector outward from the center of curvature of the curvature of the filament at s.

The outer solution in the limit $r \to 0$ at the point s on the line filament is a sum of three terms:

(1) The cut-off integral (2.1) obtained by the application of the Biot-Savart law.

(2) An asymptotic ($r \to 0$) solution for the missing curved segment of the vortex filament. This is found by subtracting from the known solution for a vortex ring (TUNG & TING, 1967) the cut-off integral representing the ring excluding the small arc (from $-l$ to l).

(3) An apparent free stream equal and opposite to the self-induced motion $\bar{q}$ at the point s. This is required to keep the filament stationary permitting a steady-flow solution of the vorticity equations to govern the motion.

In WIDNALL, BLISS and ZALAY (1970), the matching of the inner and outer solutions was done using the vertical velocity u. The u velocity from the small arc segment in the limit $r \to 0$ can be shown to be

$$\lim_{r\to 0} u_{-l,\,l} \approx \frac{\Gamma}{2\pi}\left\{-\frac{\sin\theta}{r} + \frac{1}{2R}\ln\frac{2l}{r} - \frac{1}{2R}\cos^2\theta\right\}, \tag{2.3}$$

where θ is the angle between r and the x-axis and R is the local radius of curvature at s.

With the addition of the cut-off integral (2.2) and the apparent free stream $-\bar{q}$, the total outer solution for the vertical velocity in the limit $r \to 0$ is

$$\lim_{r\to 0} u^0 \approx \frac{\Gamma}{2\pi}\left|-\frac{\sin\theta}{r}+\frac{1}{2R}\ln\frac{2l}{r}-\frac{1}{2R}\cos^2\theta+\frac{1}{2}\left\{-\ln\frac{l}{R}+\bar{B}(s)\cdot\bar{n}\right\}\right|-\bar{q}\cdot\bar{n},$$

where $\bar{n}$ is the unit binormal to the filament.

To find a solution valid in the immediate neighborhood of the rotational vortex core, it is advantageous to work in a coordinate system moving with the local velocity of the core. At the outset, this velocity is unknown. The local solution to the conservation equations of mass and vorticity plus the effects of distant elements of the vortex filament determine the necessary self-induced motion. Prior to a small bending perturbation, the initial swirl and axial profiles of the vortex core will be assumed to have radial symmetry.

Both the equation of conservation of mass

$$\nabla\cdot\mathbf{Q}=0 \tag{2.5}$$

and the definition of vorticity

$$\boldsymbol{\Omega}=\nabla\times\mathbf{Q} \tag{2.6}$$

are kinematic conditions for the velocity and vorticity fields. In the dynamic equation of vorticity, one must consider that any rotation of the coordinate system moving with the vortex will introduce an apparent vorticity.

The solution procedure is most straightforward if the coordinate system is chosen to account for the local curvature of the vortex line: the center of the vortex line is located at a radial coordinate, ϱ, equal to the local radius of curvature R; the polar system, ϱ and ϕ, lies in the local oscillating plane of the vortex line; the z coordinate is parallel to the local binormal of the vortex line. In the analysis, a local r, θ, s curvilinear system, attached to the head of the R vector, is used with all lengths normalized by R.

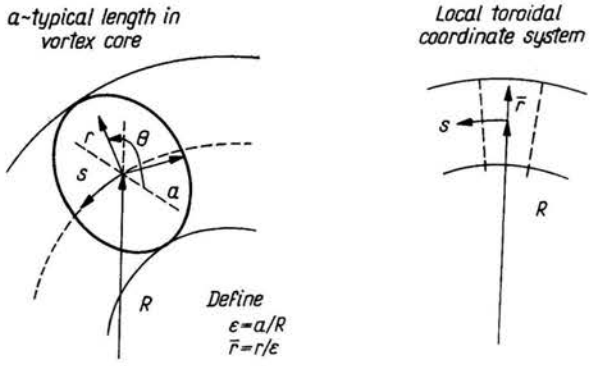

FIG. 1. Local coordinate system for a curved vortex.

In the r, θ, s coordinates (Fig. 1), the appropriate length scale for changes along the vortex is $s \sim 0$ [1], while the appropriate length scale for changes within the cross-section of the vortex core is $r \sim 0$ [ε]. To identify the proper balance between these changes within and near the vortex core, the variable $\bar{r} = r/\varepsilon$ is introduced. The local geometry of a curved vortex tube is sketched in Fig. 1

Although viscous forces play a role in determining the swirl and axial velocity profiles of the unperturbed vortex filament, a detailed analysis of the appropriate time scales for the instability shows that the perturbation problem may be treated as inviscid. Also, the slight variation of vortex properties along the core due to viscous forces may be ignored. (See BLISS, 1970.)

With these simplifications, the dynamic equation of vorticity becomes

$$\mathbf{Q}\cdot\nabla\boldsymbol{\Omega} = \boldsymbol{\Omega}\cdot\nabla\mathbf{Q} \tag{2.7}$$

merely relating changes in vorticity to stretching and convection.

To determine the effect of curvature on the flow within and near the vortex core, a solution will be sought in the form of an expansion in the small parameter $\varepsilon = a/R$.

$$\begin{aligned}\bar{\mathbf{Q}} &= \bar{\mathbf{Q}}_0+\varepsilon\bar{\mathbf{Q}}_1+\varepsilon^2\bar{\mathbf{Q}}_2+\cdots\\ \bar{\boldsymbol{\Omega}} &= \bar{\boldsymbol{\Omega}}_0+\varepsilon\bar{\boldsymbol{\Omega}}_1+\varepsilon^2\bar{\boldsymbol{\Omega}}_2+\cdots,\end{aligned} \tag{2.8}$$

where the components of the velocity and vorticity vectors are

$$\bar{\mathbf{Q}} = u\bar{i}_r+v\bar{i}_\theta+w\bar{i}_z, \tag{2.9}$$

$$\bar{\boldsymbol{\Omega}} = \xi\bar{i}_r+\eta\bar{i}_\theta+\zeta\bar{i}_z. \tag{2.10}$$

The velocity and vorticity are non-dimensionalized by $\Gamma/2\pi a$ and $\Gamma/2\pi a^2$, respectively.

$\mathbf{Q}$ and $\boldsymbol{\Omega}_0$ are the velocity and vorticity of the straight vortex, $v_0(r)$ is the initial swirl velocity, $w_0(r)$ is the initial axial velocity; the initial radial components, u_0 and ξ_0, are zero. The initial components of vorticity are

$$\zeta_0 = \frac{1}{r}\frac{\partial(rv_0)}{\partial r}, \qquad \eta_0 = -\frac{\partial w_0}{\partial r}. \tag{2.11}$$

$\mathbf{Q}_1$ and $\boldsymbol{\Omega}_1$ are the-first order perturbations in velocity and vorticity due to curvature.

The expansion (2.8) is substituted into the governing equations and terms with equal powers of ε are equated. The lowest order equations confirm (2.11). The next order terms give the governing equations for $\bar{\mathbf{Q}}_1$ and $\boldsymbol{\Omega}_1$. The process is straightforward but cumbersome; the final results can be understood as the effects of the stretching and tilting of the vortex filaments due to curvature and the requirements of conservation of mass in the deformed vortex cross-section. (We refer to BLISS (1970) for details.) The resulting equation of conservation of mass becomes

$$\frac{\partial u_1}{\partial r}+\frac{u_1}{r}+\frac{1}{\bar{r}}\frac{\partial v_1}{\partial\theta}+v_0\cos\theta = 0. \tag{2.12}$$

From (2.12), we see that to this order, the effect of axial velocity does not appear in the equation for conservation of mass. This allows the use of a stream function ψ related to the velocity field by

$$u = \frac{1}{1+\varepsilon\bar{r}\sin\theta}\frac{1}{\bar{r}}\frac{\partial\psi}{\partial\theta} \quad \text{and} \quad v = \frac{-1}{1+\varepsilon\bar{r}\sin\theta}\frac{\partial\psi}{\partial\bar{r}}. \tag{2.13}$$

(The scale for non-dimensionalizing ψ is $\Gamma/2\pi R$.) The expansion for ψ is

$$\psi = \psi_0(\bar{r}) + \varepsilon\psi_1(\bar{r}, \theta) + \ldots \tag{2.14}$$

The appropriate θ dependence of ψ_1 is

$$\psi_1 = \hat{\psi}_1(\bar{r})\sin\theta, \tag{2.15}$$

where $\hat{\psi}_1 = r\hat{u}_1(\bar{r})$.

The ordinary differential equation that governs $\hat{\psi}_1$ is obtained by introducing the stream function directly into the equation of vorticity conservation and into the definition of vorticity, eliminating vorticity between them.

The result is

$$\frac{d^2\hat{\psi}_1}{d\bar{r}} + \frac{1}{\bar{r}}\frac{d\hat{\psi}_1}{d\bar{r}} - \left(\frac{d^2v_0}{d\bar{r}^2} + \frac{1}{\bar{r}}\frac{\partial v_0}{\partial\bar{r}}\right)\frac{\hat{\psi}_1}{v_0} = -2\bar{r}\left(\zeta_0 - \frac{w_0\eta_0}{v_0}\right) - v_0 . \tag{2.16}$$

The equation determines perturbation vorticity ζ_1 due to three non-homogeneous source terms involving the initial velocity and vorticity distribution: the first is due to stretching of ζ_0, the second is due to tilting of η_0, the last is due to changes in swirl velocity required by mass conservation. By inspection, one solution to the homogeneous equation is found to be $\hat{\psi}_1 = v_0$. Once one homogeneous solution of a second-order ordinary differential equation is known the complete solution can be found.

With the requirement that the velocity in the core be everywhere finite, the solution can be written in terms of definite integrals.

$$\hat{\psi}_1 = C_1 v_0 - \frac{1}{2}\bar{r}^2 v_0 - v_0\int_0^{\bar{r}}\frac{1}{\bar{r}v_0^2}\left(\int_0^{\bar{r}}\bar{r}v_0\,d\bar{r}\right)d\bar{r} - v_0\int_0^{\bar{r}}\frac{1}{\bar{r}v_0^2}\left(\int_0^{\bar{r}}\bar{r}^2\frac{d(w_0)}{d\bar{r}}\,d\bar{r}\right)d\bar{r}. \tag{2.17}$$

Now that $\hat{\psi}_1$ is known, the perturbations in velocity and vorticity, $\mathbf{Q}_1$ and $\boldsymbol{\Omega}_1$ can be determined. The general solution for the flow within and near a perturbed vortex core has now been obtained. If one wished to work out the streamline pattern and velocities for a particular initial vorticity distribution, the integrals in (2.17) would have to be evaluated.

However, the details of the vorticity distribution affect the self-induced motion only through the velocity field "seen" by the vortex at distances larger than the core radius, i.e., as $\bar{r} \to \infty$.

In the outer limit $\bar{r} \to \infty$, the vertical velocity obtained from this solution is

$$\lim_{r/\varepsilon\to\infty} u^i \simeq \frac{\Gamma}{2\pi R}\left[-\frac{\sin\theta}{r} + \frac{1}{2}\left\{\ln\frac{a}{r} - \ln R - \left(A - C - \frac{1}{2}\right) - \cos^2\theta\right\}\right], \tag{2.18}$$

where

$$A = \lim_{r/a\to\infty}\left(\int_0^{r/a} rv_0^2\,dr - \ln r/a\right) \tag{2.19}_1$$

and

$$C = 2\int_0^{\infty}\bar{r}w_0^2\,dr . \tag{2.19}_2$$

The parameters A and C evidently contain all the effects of the details of both vorticity and axial velocity distribution. The interpretation of C is quite simple; C is proportional to twice the kinetic energy or the momentum flux in the axial flow. The interpretation of A is more subtle; the first integral in $(2.19)_1$ expresses the behavior of the total kinetic energy of the swirl motion for the fluid within $\bar{r}$. However, the kinetic energy of a single point vortex is singular as $\log \bar{r}$ as $\bar{r} \to \infty$. The singular part depends only upon $\bar{r}$; the finite part A depends upon the details of the swirl distribution. For a vortex core of constant vorticity $A = 1/4$; for a decaying line vortex, $A = -.058$

When the asymptotic matching principle,

$$\lim_{r/\epsilon \to \infty} u^i - \lim_{r \to 0} u^0,$$

is applied, the following expression for the self-induced motion $\bar{q}(s)$ is obtained:

$$\bar{q}(s) \approx \frac{\Gamma}{4\pi R(s)} \left[\left(-\ln \frac{a}{2R(s)} + A - C - \frac{1}{2} \right) \bar{n} + \bar{B}(s) \right]. \tag{2.20}$$

Comparison of the induced velocities from (2.2) and (2.20) shows that the correct induced velocity is obtained if the cut-off distance l is chosen so that

$$\ln l = \ln \frac{a}{2} + \frac{1}{2} - A + C. \tag{2.21}$$

This general formula for cut-off distance has been applied in several problems: the calculation of the self-induced motion of a vortex ring and of a sinusoidally perturbed vortex line; the study of the vortex pair instability; the study of the instability of the vortex ring and of helical vortex filaments. The restrictions on the application of this formula and the concept of cut-off distance are that the core size be smaller than both the local radius of curvature and the wave length of disturbances along the filament. (It will be seen that the instability of the vortex ring occurs for wavelengths which do not comfortably meet this requiremen.)

Specific applications of this formula to the vortex ring and the sinusoidally perturbed vortex filament give the following results. The sinusoid rotates rigidly (without change of shape) with a constant angular velocity

$$\Omega_p = \frac{\Gamma}{4\pi} k^2 \left[\ln \frac{1}{ka} + A - C + (\ln 2 - \gamma) \right] \tag{2.22}$$

in a direction opposite to the rotation of flow in the vortex core.

The propagation velocity of the ring is

$$u_p = \frac{\Gamma}{4\pi R} \left[\ln \frac{8R}{a} + A - C - \frac{1}{2} \right], \tag{2.23}$$

where in both cases a is the characteristic dimension of the vortex core. (A vortex ring containing an axial flow is possibly only of academic interest.)

In both of these applications, the presence of an axial velocity will reduce the speed of rotation or propagation. This result has a very simple physical interpretation. To contain the momentum flux (the integral) within the vortex core, an inward force, acting upon the

filament, of magnitude

$$F = -\int_0^\infty 2\pi r w^2 \, dr/R \tag{2.24}$$

is required, where R is the local radius of curvature. This force is provided by a Kutta-Joukowski lift acting upon the vortex cross-section whenever the velocity of the ring differs from the basic self-induced velocity for a filament without axial flow U_0. The lift on the filament is then

$$\Gamma(U_p - U_{po}). \tag{2.25}$$

A combination of (2.24) and (2.25) confirms that the ring slows down to provide the lift force necessary to contain the internal flow. (This result, of course, has limitations: it is unlikely that the ring would ever reverse its direction, and it is also obvious that the ring would be unable to contain the axial flow as the flow velocity becomes large. The ring would probably become unstable.)

This simple force/momentum flux balance confirms the result already obtained by a rather lengthy analysis (and a fortuitous solution, by inspection, of the perturbed vorticity equations.) This suggests that an understanding of the motion and stability of vortex filaments containing axial flow may be obtained by an application of some rather simple ideas of lift on a vortex cross-section and momentum flux in a perturbed cylindrical duct by means of slender body theory, which is valid for $ka \ll 1$, an approximation already inherent in most treatments of vortex filaments.

These ideas were exploited by WIDNALL and BLISS (1971) in a slender-body analysis of the motion and stability of vortex filaments containing axial flow. This study found that such a flow would become unstable for wavenumbers $\frac{k\overline{w}}{\Omega} > \sqrt{2}-1$, where $\overline{w}$ is the axial velocity and Ω is the angular velocity of the vortex core.

3. The stability of vortex rings

The investigation of the stability of a slender-filament vortex ring to small sinusoidal displacements of its centerline proceeds by evaluating the self-induced velocities at the filament due to these perturbations. These induced velocities then determine the resulting motion of the filament and thus the growth rate (if any) of the perturbations

$$\bar{q}(y) = \frac{\Gamma}{4\pi}\int_c \frac{(\bar{y}-\bar{y}_1)\times d\bar{y}}{|\bar{y}-\bar{y}_1|^3}. \tag{3.1}$$

The perturbations of the vortex filament ring are taken as sinusoidal displacements in both the radial and axial directions. (For the linearized stability problem, tangential displacements are not considered.) In a coordinate system moving with the velocity of the unperturbed vortex ring V_0, the Cartesian components of the vector y to a point on the perturbed vortex filament (Fig. 2) are

$$\begin{aligned} y_1 &= (R+\varrho_0 e^{in\theta})\cos\theta, \\ y_2 &= (R+\varrho_0 e^{in\theta})\sin\theta, \\ y_3 &= \xi_0 e^{in\theta}, \end{aligned} \tag{3.2}$$

where ϱ_0 and ξ_0 are the perturbation amplitudes. The wavenumber n is an integer. To calculate the resulting motion of a point y_1 on the filament, it is convenient to express all vectors in components of the local polar unit vectors $\bar{i}_{r_1}$, and $\bar{i}_{\theta_1}$ and $\bar{k}$ at $\bar{y}_1$ as

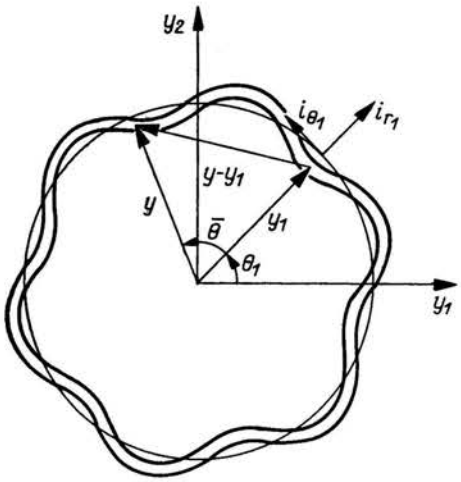

FIG. 2. Configuration and coordinate system for the sinusoidal perturbation of a vortex-filament ring.

sketched in Fig. 2. In these coordinates, the distance to the point y_1 on the perturbed filament is

$$\bar{y}_1 = (R+\varrho_0 e^{in\theta_1})\bar{i}_{r_1}+\xi_0 e^{in\theta_1}\bar{k}. \tag{3.3}$$

Since the vortex element moves with the self-induced velocity $q(y)$ from (1), the kinematic equation of motion of the point $\bar{y}_1$ is just

$$\frac{d\bar{y}_t}{dt} = \frac{d\bar{y}_1}{dt}+V_0\bar{k} = \bar{q}(\bar{y}_1), \tag{3.4}$$

where $\bar{y}_t$ is distance measured in a fixed coordinate system.

The self-induced velocity in the radial and axial directions at the point $\bar{y}_1$ (from (1)) is of the general form

$$\bar{q} = V_0\bar{k}+\xi_0 e^{in\theta_1}V_{\xi 0}\bar{i}_{r_1}+\varrho_0 e^{in\theta_1}V_{\varrho 0}\bar{k}, \tag{3.5}$$

that is, ξ_0 displacements induce a radial velocity and ϱ_0 displacements induce an axial velocity.

From (3.3), (3.4) and (3.5), the equations for the growth of the perturbation amplitudes are then

$$d\varrho_0/dt = V_{\xi 0}\xi_0, \tag{3.6}_1$$

$$d\xi_0/dt = V_{\varrho 0}\varrho_0. \tag{3.6}_2$$

Assuming a solution of the form $\varrho_0(t) \approx e^{\alpha t}$, we obtain an eigenvalue problem for the amplification rate α

$$\begin{bmatrix} \alpha & -V_\varrho \\ -V_{\xi 0} & \alpha \end{bmatrix}\begin{Bmatrix} \xi_0 \\ \varrho_0 \end{Bmatrix} = 0. \tag{3.7}$$

The eigenvalue α is then

$$\alpha = \sqrt{(V_{\varrho 0} V_{\xi 0})}. \tag{3.8}$$

When α is real, the small perturbation on the vortex ring grows exponentially; if α is imaginary, the perturbation rotates around (not along) the filament.

$V_{\varrho 0}$ and $V_{\xi 0}$ which determine the amplification α are found by a proper interpretation of (3.1) in terms of the general formula for cut-off (2.21).

Unless n is large, in the limit of very small core size $a \to 0$ the dominant terms in (3.1) are proportional to $\ln(a/R)$ and are given by

$$V_{\xi 0} \approx \frac{\Gamma}{4\pi R^2} n^2 \ln(a/R), \tag{3.9}$$

$$V_{\varrho 0} \approx (\Gamma/4\pi R^2)(1-n^2)\ln(a/R). \tag{3.10}$$

The factors n^2 and n^2-1 are proportional to the changes in local curvature due to the ξ_0 and ϱ_0 displacements. These expressions have been used by J. J. THOMSON (1883) and others to study the stability of a vortex ring to sinusoidal perturbations. In this case, the amplification rate is

$$\alpha \approx (\Gamma/4\pi R^2) n \sqrt{(1-n^2)\ln(a/R)}. \tag{3.11}$$

In this limit ($a \to 0$), the ring is neutrally stable; each mode (n) has a definite frequency of oscillation. (This frequency is zero for $n = 0, 1$.)

For a complete investigation of the stability of the vortex ring, however, the full expression for $V_{\varrho 0}$ and $V_{\xi 0}$ should be used, since for larger values of a and n the numerical values of $\ln(a)$ and $\ln(n)$ are essentially 0(1). This is the extension made in WIDNALL and SULLIVAN (1973) to the previous work.

Before presenting the results of this stability calculation, it is important to consider how to characterize the effects of the vorticity distribution within the core upon the stability of the ring and how to model the effects of changes in the vortex core radius as a result of the perturbation.

Both the self-induced translational velocity of the ring V_0 and the induced velocities due to the perturbations are influenced by the details of vortex core size and vorticity distribution only through the combination $-\ln(a/R)+A$. Dividing V_0 by $\Gamma/4\pi R$ gives a parameter $\tilde{V}$ that is a function only of this combination

$$\tilde{V} = \frac{V_0}{\Gamma/4\pi R} = \ln\frac{8R}{a} + A - \frac{1}{2}. \tag{3.12}$$

Therefore, for the purposes of the stability calculation, $\tilde{V}$ completely characterizes the vortex ring. In an experimental situation, it is also much easier to measure $\tilde{V}$ than both a and A. Some typical values of $\tilde{V}$ are: for a vortex ring of uniform vorticity with a core radius $a/R = 0.1$, $V = 4.13$; for Hill's spherical vortex, $V = 1.8$ (The effective radius is taken as the radius to the point of zero velocity within the ring, $R/\sqrt{2}$.) This value is also obtained for a ring of uniform vorticity if a/R is set equal to 1, obviously outside the region of validity

for slender vortex filament theory. The amplification rate α is non-dimensionalized by the parameter $\Gamma/4\pi R^2$ to obtain

$$\bar{\alpha}(\tilde{V}; n) = \frac{\alpha}{\Gamma/4\pi R^2}.$$

For a given n, $\bar{\alpha}$ is a function of $\tilde{V}$ only. If the amplification rate α is multiplied by R/V_0 (the time to travel one radius), the non-dimensional spatial amplification α_x is obtained. For a given n, α_x is a function of $\tilde{V}$ only. The relation between α_x and $\bar{\alpha}$ is

$$\alpha_x(\tilde{V}; n) = \frac{\alpha R}{V_0} = \frac{\bar{\alpha}(\tilde{V}; n)}{\tilde{V}}. \tag{3.13}$$

This quantity will be calculated numerically for various n using (3.8).

WIDNALL and SULLIVAN (1973) considered two simple models to predict the local core radius along the perturbed filament. One assumes that variations in the core size along the filament will be resisted by very small scale process within the core, i.e., flow along the filament due to changes in the interior pressure produced by changes in core size. In this case, a is taken as a_0 (for $n \neq 0$ there is no change in length of the filament to $O(\varrho_0/R)$). The other model assumes that the filament will conserve volume locally so that $a^2(s)l(s)$ remains constant along the filament during the perturbation. In this case, a at a point on the filament is (approximately)

$$a \approx a_0 \left| 1 - \frac{1}{2}\frac{\varrho_0}{2R_1} e^{in\theta_1} \right|,$$

so that

$$\ln \frac{a}{R} \approx \ln \frac{a_0}{R} - \frac{1}{2}\frac{\varrho_0}{2R} e^{in\theta_1}.$$

The numerical results (spatial amplification rate α_x (3.13)) as a function of non-dimensional translational velocity $\tilde{V}$ (3.12) are shown in Fig. 3 for the two models of the

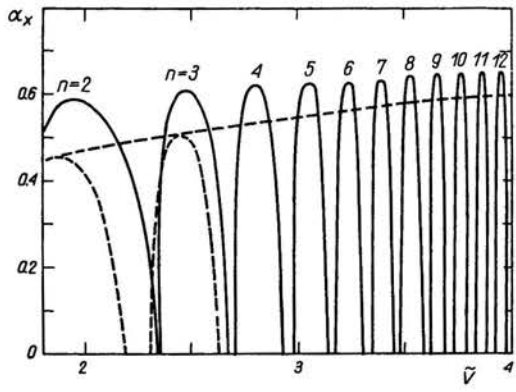

FIG. 3. Non-dimensional spatial amplification rate α_x of the vortex ring instability as a function of V and mode number n; ——, constant-core-radius model; – – –, constant-local-volume model (Only the envelope is shown for $n \geqslant 4$).

behavior of the vortex core during deformation. For each mode of deformation, n waves around the perimeter ($n \geqslant 2$), there is a region of $\tilde{V}$ for which α_x is real and positive (instability.) For large V (small core size), the unstable mode contains many wavelengths. This makes it more difficult to justify the application of the asymptotic solution, since in this

analysis the core size is required to be small by comparison to both the radius of the ring and the wavelength of the disturbance. However, one can expect the asymptotic solution to be at least qualitatively valid outside its limits. Also, the results of the analysis would not be expected to hold near $\tilde{V} = 1.8$, the value for the Hill's spherical vortex, but the results may give an indication of what happens in that limit.

The amplification α_x and the range of $\tilde{V}$ for which a given mode (n) is unstable seems to be only slightly affected by the behavior of the vortex core size during the deformation.

To determine, at least qualitatively, whether the instability would actually be observed, viscous effects can be introduced into the determination of core size. The actual time that a given vortex filament remains within the band of instability of a particular mode (n) depends on the viscous growth of the core. Both the core radius a and $\tilde{a}$ ($\tilde{a} \propto a/R$) vary as

$$a \propto R\tilde{a} \propto \sqrt{(\nu t)}, \tag{3.15}$$

where t is taken from some effective origin since filaments are formed by a roll-up process and have a finite core at $t = 0$.

The time, Δt, spent in the range of core size a to a plus Δa is then given by

$$\Delta t \propto \frac{\Delta\tilde{\alpha} \cdot \tilde{\alpha} R^2}{\nu}. \tag{3.16}$$

A measure of total amplification is $\alpha \Delta t$ given by

$$\alpha \Delta t \propto (\Gamma/n\nu) \ln(n) \Delta\tilde{a} \cdot \tilde{a}. \tag{3.17}$$

This suggests that if the Reynolds number ($\mathrm{Re} = \Gamma/n\nu$) is small, one is not apt to observe vortex ring instability since a sufficient amplification of a given unstable mode may not occur before the properties of the core change, so that the mode becomes neutrally stable.

4. Experimental study of vortex rings

The preceding analysis shows that both the propagation velocity of a vortex ring (2.23) and its stability depend upon the details of the distribution of vorticity within the core only through the parameter A. An experiment to determine the structure of the ring was reported in SULLIVAN, WIDNALL and EZEKIEL (1973); the experiments on stability were reported in WIDNALL and SULLIVAN (1973). These experiments consisted of laser Doppler velocimeter (L.D.V.) measurements to determine the axial and radial velocity distributions and the total circulation of the ring. Flow visualization studies to determine the ring radius and speed and the mode and amplification rate of the instability were also carried out. The vortex rings were generated by pulsing air through a sharp-edged orifice using a loudspeaker. The circulation and core size were controlled by the amplitude and the duration of the electric-signal to the loudspeaker.

Measurements of the axial and radial velocity distributions in vortex rings were made using a two-component laser Doppler velocimeter. The experimental layout with only a one-component LDV system drawn for clarity is shown in Fig. 4. The LDV, which is a dual scatter system, measures the Doppler shift of laser light scattered from particles

in the flow-field. In the present experiment, the particles are 2.0μ diameter oil particles estimated to have a velocity within 0.5% of the fluid velocity. The actual two-dimensional system used is constructed by adding a second beam-splitter (rotated 90° with respect to the first) to form four parallel beams in a diamond pattern. Further details of the system and the experimental techniques appear in SULLIVAN, WIDNALL and EZEKIEL (1973).

Detailed surveys of a relatively thick core ring (denoted Ring No. 1) and a thin core ring (Ring No. 2) were made. Complete two-dimensional data were taken for Ring No. 1

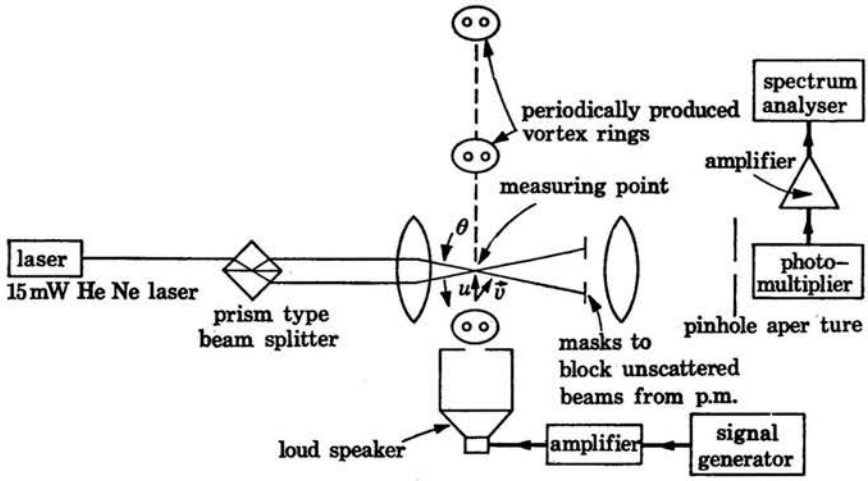

FIG. 4. One-dimensional dual scatter LDV system.

but only the component of velocity in the direction of ring travel was measured for Ring No. 2.

The total circulation was determined by an integration of the axial velocity along the centerline.

A summary of the data is given in Table 1. The non-dimensional parameter $\tilde{V}$ (3.12) which characterizes the core size and vorticity distribution was calculated from the measured circulation, ring speed and radius

$$\tilde{V} = \frac{\bar{v}_0}{\Gamma/4\pi R}.$$

Table 1. Data summary

	r_0(ft)	U_0(ft/s)	Γ_0(ft²/s)	a/r_0	$\tilde{V}$	Re = Γ/ν
Ring No. 1	0.091	2.60	1.21	0.27	2.46	7 780
Ring No. 2	0.111	13.5	6.07	0.075	3.10	37 900

Since both components of velocity were measured on Ring No. 1, the vorticity distribution throughout the vortex ring can be found. In order to minimize differentiation of data, the fact that ω/r is constant on a streamline for a steady axisymmetric flow is utilized.

The streamlines are found for the entire flowfield and the value of ω is calculated only along $z/r_0 = 0$ giving a value of ω on each streamline, so ω is known everywhere.

Integration of velocity along convenient curves gives the streamfunction ψ, so that the streamlines, lines of constant ψ, can be plotted. These streamlines are shown superposed on a strobe photograph of Ring No. 1 in Fig. 5.

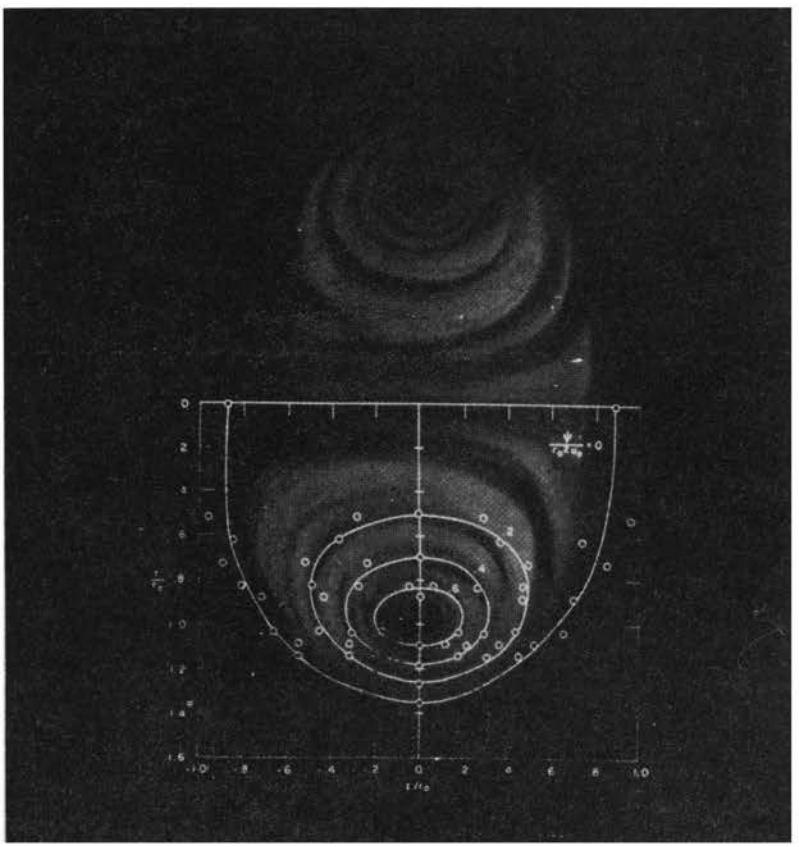

FIG. 5. Side view of ring No. 1 with measured streamlines superposed.

The vorticity, ω, is calculated along $z = 0$ differentiating the data

$$\frac{\omega(r, 0)}{(U_0/r_0)} = \frac{\partial\left(\frac{V}{U_0}\right)}{\partial\left(\frac{z}{r_0}\right)}\bigg|_{z=0} - \frac{\partial\left(\frac{U}{U_0}\right)}{\partial\left(\frac{r}{r_0}\right)}\bigg|_{z=0}.$$

The vorticity distribution along $z = 0$ (Fig. 6) shows the expected concentration of vorticity in the core.

Using the fact that δ/r is constant on streamlines in conjunction with Figs. 5 and 6, the vorticity at any point in the ring can be found. It is estimated that for this ring roughly 85% of the vorticity is within the $\psi/R^2V_0 = .4$ streamline.

The non-dimensional ring velocity $\tilde{V}$ can also be determined from the measured vorticity. The non-dimensional self-induced velocity of a vortex ring with an arbitrary distribution of vorticity is given by

$$V_0 = \ln\frac{8R}{a} + A - \frac{1}{2} = \ln 8 - \frac{1}{2} + (A - \ln a/R),$$

where

$$A = \lim_{\bar{r}\to\infty} \int_0^{\infty} \hat{v}_0^2(\bar{r})\bar{r}\,d\bar{r} - \ln\bar{r};$$

$\hat{v}_0$ is the non-dimensional swirl velocity (in ϱ, θ coordinate system) $\hat{v}_0 = v_0 2\pi a/\Gamma$ and $\bar{r} = ra/R$, where a is some typical dimension in the vortex core. (Actually, the parameter $A - \ln a/R$ is independent of the choice of length scale.)

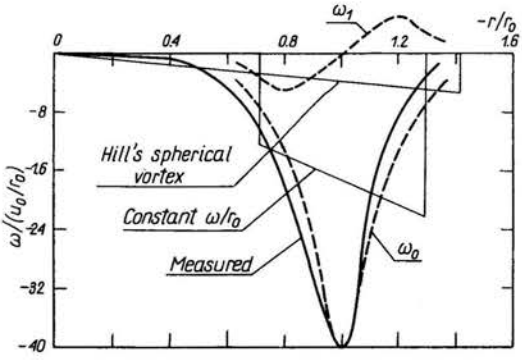

FIG. 6. Vorticity $\omega/V_0/R$, versus r/R along $z/R = 0$.

Straightforward manipulation yields a formula for the group $A - \ln a/R$ in terms of the zeroth-order vorticity ζ_0, the results being

$$A - \ln\frac{a}{R} = \frac{-2\int_0^{\infty} \bar{r}\zeta_0(\bar{r}) \ln\bar{r} \int_0^{\bar{r}} \bar{r}'\zeta_0(\bar{r}')\,d\bar{r}'\,d\bar{r}}{\left[\int_0^{\infty} \bar{r}\zeta_0(\bar{r})\,d\bar{r}\right]^2}.$$

If the vorticity is uniform within a radius $r = a$, this expression gives the familiar result $A = 1/4$.

Direct numerical integration of this formula using the values of δ_0 obtained from the measured vorticity gives $\tilde{V} = 3.01$ as compared with a measured value of 2.46, an error of 20%. Since the ratio of core size to radius is about 0.27, perhaps a 20% discrepancy between experiment and an asymptotic theory which assumes $a/R \ll 1$ is not surprising.

Multiple-flash strobe pictures were taken to determine the ring speed and the general features of the vortex-ring instability. In some cases, the ring appeared to completely disintegrate as a result of the instability; in other cases, however, a new ring with a slower speed is formed after the initial instability (also observed by both KRUZTSCH (1939) MAXWORTHY (1972)). Single-flash strobe pictures were used to determine the radius of the ring and the number of unstable waves. The amplification rates were measured directly from

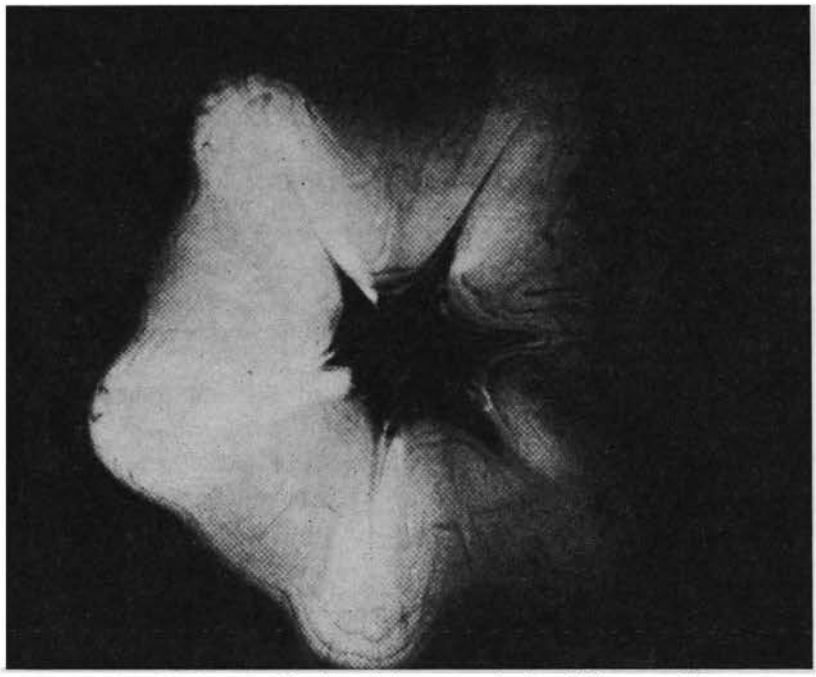

FIG. 7. Flow visualization of the vortex ring instability; $n = 6$.

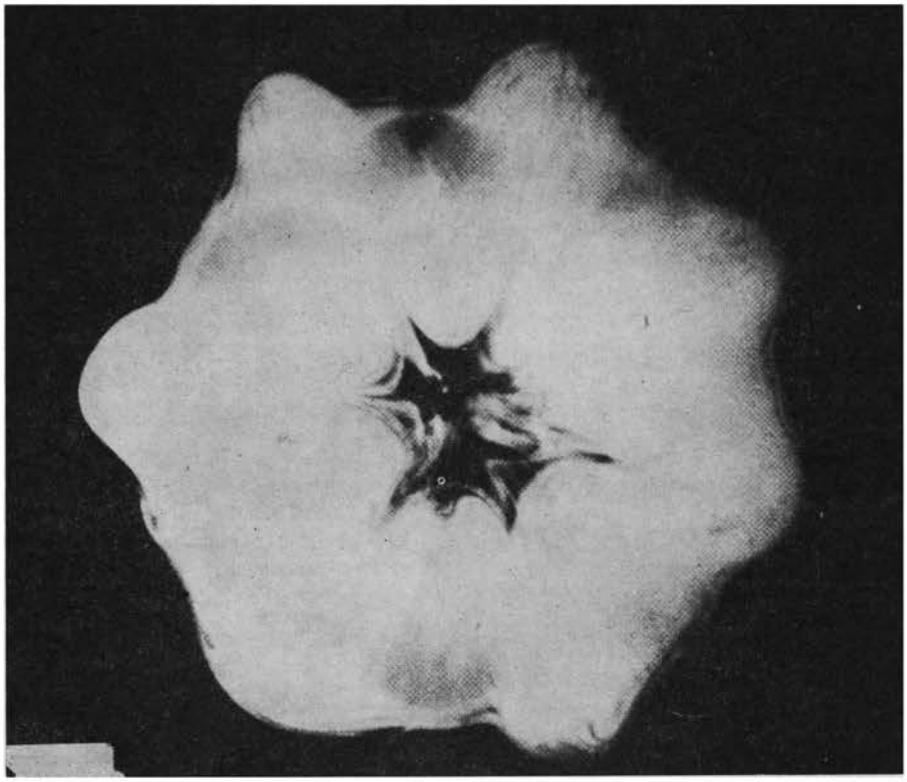

FIG. 8. Flow visualization of the vortex ring instability; $n = 7$.

the frames of strobe motion pictures. Figures 7 and 8 are front-view strobe pictures of the $n = 6$ and $n = 7$ mode instability. Since smoke particles do not diffuse into the vortex core, it can be seen as a dark band in these photographs.

These experimental observations are very similar to those of KRUZTSCH (1939) who presented experimental results for the unstable mode number n as a function of the velocity and radius of the ring.

5. Comparison between theory and experiment results for vortex rings

Two comparisons can be made between the experimental results and theoretical analysis: firstly, for a given vortex core size and vorticity distribution, a comparison of the unstable mode (n) as observed with that predicted; secondly, a comparison of the actual amplification rate of the instability in the early stages of growth with the prediction of the linear stability analysis.

Table 2. Data summary

n	R/cm	V_0/cm s^{-1}	Γ/cm^2 s^{-1}	$\tilde{V}$	Re $= \Gamma/\nu$	$a^{(1)}$/cm	a/R
6	2.17	79.2	855	2.52	5 790	—	—
7	2.77	79.2	1124	2.46	7 780	0.826	0.34
8	3.17	70.4	1013	2.77	6 800	—	—
12	3.32	50.5	6717	3.16	45 200	0.424	0.14

(1) Defined as distance from core center to peak tangential velocity (see SULLIVAN, 1973).

From the experimental measurement of V_0, Γ and R, the parameter $\tilde{V}$ is formed (Table 2). The actual observed mode number n of the instability is shown in Fig. 9 as a function of $\tilde{V}$. Also shown is the value of n that is predicted to be the most unstable for

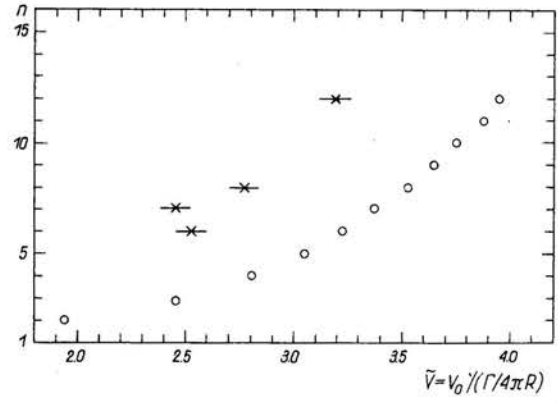

FIG. 9. Number of waves in the unstable mode as a function of $V = V_0/\Gamma(4\pi R)$; ×-experiment; ○-theoretical prediction at maximum amplification, V from measured vorticity.

the value of $\tilde{V}$. Although the trend of increasing n with increasing $\tilde{V}$ (decreasing core size) is in agreement with the theoretical predictions, the actual values of n against $\tilde{V}$ are not in good agreement. This is most likely due to the fact that the ratio of wavelength to vortex core radius of the unstable mode is not small as required by the asymptotic theory.

However, when the value of V_0 is determined directly from measured vorticity rather than circulation (as described in 4.), much better agreement is obtained. This indicates that perhaps the disagreement exists between the predicted and observed self-induced velocity of the ring.

The measured radial perturbation of the ring due to the instability as a function of time is shown in Fig. 10. The growth of the perturbation during the early stages of the instability shows good agreement with the theoretical predictions. This is due in part to the fact that the amplification rate for an unstable mode is insensitive to both $\tilde{V}$ and modal number n.

Both the linear stability analysis and the experiments carried out at moderately high Reynolds numbers show that the vortex ring is unstable to sinusoidal displacements of the vortex filament. The number of waves around the perimeter increases with decreasing vortex core size. These results indicate that laboratory experiments at lower Reynolds numbers should be interpreted with caution since analysis indicates that viscous effects can stabilize the ring.

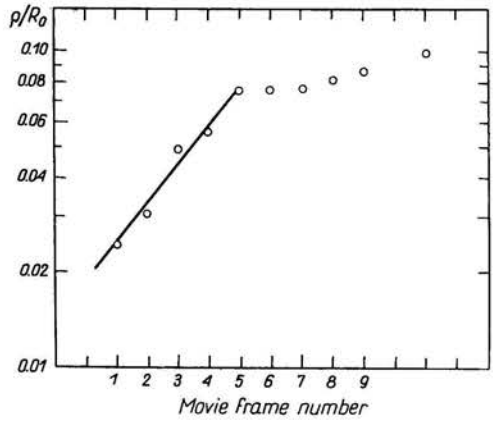

FIG. 10. Percentage radial perturbation for the vortex ring of Fig. 8 measured at each strobe movie frame (time between frames 14.5ms); ——, exponential growth $\alpha_x = 0.69$; theoretical prediction, $\alpha_x = 0.64$.

This investigation has raised many questions. If the analysis of the self-induced motion due to bending a vortex filament was carried to higher order in the ratio of vortex-core radius to perturbation wavelength, better agreement between theory and experiment might be obtained. Alternatively, a full three-dimensional small-perturbation solution to the vorticity equations for a particular initial vorticity distribution (without the simplifying assumptions of the asymptotic theory) may be required. Detailed examination of the flow field would be required to investigate all of the effects of the instability on the vortex ring such as the suggestion that under some conditions, vorticity is shed and a new ring is formed.

References

1. D. B. BLISS, *The dynamics of curved rotational voertex lines*, M. S. Thesis, Massachusetts Institute of Technology, 1970.
2. S. C. CROW, *Stability theory for a pair of trailing vortices*, AIAA, Paper No. 70–53, 1970.
3. F. W. DYSON, *The potential of an anchor ring*, Phil. Trans. A. CLXXXIV, 1893.

4. L. E. FRAENKEL, *Examples of steady vortex rings of small cross-section in an ideal fluid*, J. F. M., **51**, 1, 1972.
5. W. M. HICKS, *Researches on the theory of vortex rings*. Part II. Phil. Trans. of the Royal Society of London, **176**, Pt. 2, 725–780, 1885.
6. C. H. KRUTZSCH, *Über eine experimentell beobachtete Erscheinung an Werbelringen bei ihrer translatorischen Bewegung in Werklechin*, Flussigkeiter Annalen Der Physik 5, Folge Band **35**, 497–523, 1939.
7. LAMB, Sir H., *Hydrodynamics*, Dover Publications, Inc., New York 1945.
8. T. MAXWORTHY, *The structure and stability of vortex rings*, J. F. M., **51**, 1, 15, 1972.
9. D. W. MOORE and P. G. SAFFMAN, *The motion of a vortex filament with axial flow*, Phil. Trans. of the Royal Soc., **272**, 1226, 403–429, 1972.
10. P. G. SAFFMAN, *The velocity of viscous vortex rings*, Studies in Applied Math, *XLIX*, 5, 370–381, 1970.
11. P. G. SAFFMAN, *The velocity of viscous vortex rings*, Aircraft Wake Turbulence and Its Detection, p. 9, Plenum Press, New York 1971.
12. J. P. SULLIVAN, *Experimental investigation of vortex rings and helicopter rotor wakes*, Ph. D. Thesis, Massachusetts Institute of Technology, 1973.
13. J. P. SULLIVAN, S. E. WIDNALL and S. EZEKIEL, *A study of vortex rings using a laser Doppler velocimeter*, AIAA Paper No. 73–105, 1973.
14. J. J. THOMSON, *A treatise on the motion of vortex rings*, MacMillan and Co., London 1883.
15. THOMSON, Sir W. (Lord Kelvin), *Mathematical and physical papers, IV*, Cambridge University Press, Cambridge, England, 1910.
16. C. TUNG and L. TING, *The motion and decay of a vortex ring*, Physics of Fluids, **10**, 5, 901–10, 1967.
17. S. E. WIDNALL, *The stability of a helical vortex filament*, JFM, **54**, 4, 641–663, 1972.
18. S. E. WIDNALL and D. B. BLISS, *Slender body analysis of the motion and stability of an isolated vortex filament*, J. F. M., **20**, Pt. 2, 335–353, 1971.
19. S. E. WIDNALL, D. B. BLISS and A. ZALAY, *Theoretical and experimental study of the stability of a vortex pair*, Aircraft Wake Turbulence and Its Detection, Plenum Press, 305, New York 1971.
20. S. E. WIDNALL and J. P. SULLIVAN, *On the stability of vortex rings*, Proc. Roy. Soc. London A. **332**, 335–353, 1973.

DEPARTMENT OF AERONAUTICS AND ASTRONAUTICS
MASSACHUSETTS INSTITUTE OF TECHNOLOGY.